

9208

NACA TN 2877

0065797



TECH LIBRARY KAFB, NM

# NATIONAL ADVISORY COMMITTEE FOR AERONAUTICS

TECHNICAL NOTE 2877

ON THE USE OF A DAMPED SINE-WAVE ELEVATOR MOTION  
FOR COMPUTING THE DESIGN MANEUVERING  
HORIZONTAL-TAIL LOAD

By Melvin Sadoff

Ames Aeronautical Laboratory  
Moffett Field, Calif.



Washington

January 1953

AFMCC

TECHNICAL NOTE

AFL 2811



---

TECHNICAL NOTE 2877

---

## ON THE USE OF A DAMPED SINE-WAVE ELEVATOR MOTION

## FOR COMPUTING THE DESIGN MANEUVERING

## HORIZONTAL-TAIL LOAD

By Melvin Sadoff

## SUMMARY

A damped sine-wave elevator motion was used as a basis for computing the design maneuvering load on the horizontal tail. Also investigated was the effect of control frequency on the tail load.

The results indicated that the maneuvering tail-load variation computed by operational methods with the assumed damped sine-wave elevator motion agreed closely with the loads computed by a method currently specified for use in the U.S. Air Force structural loading requirements. This close agreement, coupled with the relative simplicity of the method using the damped sine-wave elevator motion, should encourage its use as an alternative procedure for computing the design maneuvering horizontal-tail load.

The maximum tail-load increments for a given design normal acceleration factor were obtained at the highest control frequency investigated indicating that a very high control frequency should be selected in computing the design maneuvering horizontal-tail load. For the practical case, however, the design control frequency may be limited by either the availability of control or by the physical or mechanical limitations with regard to control rate of the pilot or boost system used.

## INTRODUCTION

Considerable attention has been given to the problem of devising a simple and rational method for computing the maneuvering horizontal-tail loads associated with abrupt elevator motions. In reference 1, a graphical integration procedure is used to determine the tail-load variation following any arbitrary elevator motion. In reference 2, a numerical integration method is used for computing the design maneuvering

tail loads associated with an elevator motion represented by several straight-line segments simulating a pull-up push-down maneuver. The latter method has been adopted in the U.S. Air Force structural loading specifications.

Although the methods described in references 1 and 2 were a considerable improvement over methods previously available, it is believed further simplification of the computational procedure may be realized by considering a damped sine-wave elevator motion in computing the design maneuvering tail load. The damped sine-wave motion is not only more representative of that applied in flight, but, with operational methods, it is also amenable to a simple and short solution.

The primary purpose of this paper is to evaluate the use of a damped sine-wave elevator motion in computing the design maneuvering horizontal-tail load. The effect of elevator motion frequency or control rate on the maneuvering tail load is also considered.

#### NOTATION

$A_1$	$1.39 \Delta\delta_{\max}$
$A_Z$	ratio of the net aerodynamic force along the airplane Z axis to the weight of the airplane.
$b$	airplane damping coefficient $\left[ \left( \frac{-Z_{\dot{\alpha}}}{mV} \right) - \left( \frac{M_{\dot{\alpha}} + M_{\dot{\theta}}}{I_y} \right) \right]$ , per second
$b_1\omega_1$	damping factor for elevator motion, per second
$C_L$	airplane lift coefficient $\left( \frac{L}{qS} \right)$
$C_{L_t}$	horizontal-tail lift coefficient $\left( \frac{L_t}{\eta_t qS_t} \right)$
$C_m$	airplane pitching-moment coefficient about center of gravity $\left( \frac{M}{qS\bar{c}} \right)$
$\bar{c}$	wing mean aerodynamic chord, feet
$C_o$	control-deflection coefficient $\left( \frac{M_{\delta}}{I_y} - \frac{M_{\dot{\theta}}Z_{\delta}}{I_y mV} \right)$ , per second per second

$C_1$	control-rate coefficient $\left(\frac{Z_0}{mV}\right)$ , per second
$g$	acceleration of gravity, feet per second per second
$h_p$	pressure altitude, feet
$I_y$	airplane pitching moment of inertia, slug feet squared
$k$	airplane spring constant $\left(\frac{-M_{\alpha}}{I_y} + \frac{Z_{\alpha} M_0}{I_y m V}\right)$ , per second per second
$K$	parameter denoting damping ratio of airplane to that of horizontal tail
$K_1$	parameter $\left(1 - \frac{d\epsilon}{d\alpha} + \frac{dC_L}{d\alpha} \frac{\rho S l_t}{2m\sqrt{\eta_t}}\right)$
$K_2$	parameter $\left[\frac{l_t}{V} \left(\frac{d\epsilon}{d\alpha} + \frac{1}{\sqrt{\eta_t}}\right)\right]$ , seconds
$K_3$	parameter $\left(\frac{d\alpha_t}{d\delta}\right)$
$K_4$	parameter $\left[\left(\frac{dC_{L_t}}{d\alpha_t}\right) \eta_t q S_t\right]$ , pounds
$l_t$	distance from airplane center of gravity to aerodynamic center of horizontal tail, feet
$L$	airplane lift, pounds
$L_t$	horizontal-tail lift, pounds
$m$	airplane mass $\left(\frac{W}{g}\right)$ , slugs
$M$	airplane pitching moment, foot-pounds
$q$	dynamic pressure, pounds per square foot
$s$	variable introduced in Laplace transform
$S$	wing area, square feet

$S_t$	horizontal-tail area, square feet
$t$	time, seconds
$V$	airplane velocity, feet per second
$W$	airplane weight, pounds
$X, Z$	standard airplane axes
$\alpha$	airplane angle of attack, radians
$\alpha_t$	horizontal-tail angle of attack, radians
$\gamma$	flight-path angle, radians
$\delta$	elevator angle, radians unless noted otherwise
$\Delta$	when preceding a symbol denotes increment from steady-state condition
$\epsilon$	downwash angle, radians
$\eta_t$	horizontal-tail efficiency factor $\left(\frac{q_t}{q}\right)$
$\theta$	angle of pitch $(\alpha + \gamma)$ , radians
$\rho$	mass density of air, slugs per cubic foot
$\omega$	airplane short period frequency, radians per second
$\omega_1$	elevator-control-motion frequency, radians per second
$C_{L\alpha}$	airplane lift-curve slope $\left(\frac{dC_L}{d\alpha}\right)$ , per radian
$(C_{L\alpha})_t$	horizontal-tail lift-curve slope $\left(\frac{dC_{L_t}}{d\alpha_t}\right)$ , per radian
$C_{L\delta}$	$\left(\frac{dC_L}{d\delta}\right)$ , per radian
$C_{m\alpha}$	$\left(\frac{dC_m}{d\alpha}\right)$ , per radian
$C_{m\delta}$	$\left(\frac{dC_m}{d\delta}\right)$ , per radian

- $M_\alpha$   $[(C_{m\alpha})qS\bar{c}]$ , foot-pounds per radian  
 $M_{\dot{\alpha}}$   $\left[ M_{qt} \left( \frac{d\epsilon}{d\alpha} \right) \right]$ , foot-pound-seconds per radian per second  
 $M_\delta$   $[(C_{m\delta})qS\bar{c}]$ , foot-pounds per radian  
 $M_{\dot{\delta}}$   $\left\{ \frac{[-\eta_t(C_{L\alpha})_t \rho V S_t l t^2]}{2} \right\}$ , foot-pound-seconds per radian per second  
 $M_q$   $(KM_{qt})$ , foot-pound-seconds per radian per second  
 $Z_\alpha$   $-[(C_{L\alpha})qS]$ , pounds per radian  
 $Z_\delta$   $-[(C_{L\delta})qS]$ , pounds per radian  
 $\dot{\theta}, \dot{\alpha}, \dot{\gamma}, \dot{\delta}$  equivalent notation for  $\left( \frac{d\theta}{dt} \right)$ ,  $\left( \frac{d\alpha}{dt} \right)$ ,  $\left( \frac{d\gamma}{dt} \right)$ , and  $\left( \frac{d\delta}{dt} \right)$   
 $\ddot{\theta}, \ddot{\alpha}, \ddot{\gamma}$  equivalent notation for  $\left( \frac{d^2\theta}{dt^2} \right)$ ,  $\left( \frac{d^2\alpha}{dt^2} \right)$ , and  $\left( \frac{d^2\gamma}{dt^2} \right)$

#### Subscripts

- geo geometric  
 $l_0$  zero lift  
 max maximum value  
 o steady-state value  
 t horizontal tail

#### METHOD OF COMPUTATION

The general procedure is to obtain the tail-load response as a function of the Laplace transform variable  $s$  by multiplying the tail-load transfer function by the Laplace transformation of the forcing function - in the present case the damped sine-wave elevator motion. The tail-load response in the  $s$  domain may be given by the relationship

$$\Delta L_t(s) = K_4 K_3 \left[ \frac{s^2 + \left(b + \frac{K_2 C_0}{K_3}\right)s + \left(k + \frac{K_1 C_0}{K_3}\right)}{s^2 + bs + k} \right] \left[ \frac{A_1 \omega_1}{s^2 + 2b_1 \omega_1 s + (1 + b_1^2) \omega_1^2} \right] \quad (1)$$

(See appendix A for derivation.) The tail-load response in the time domain or the inverse transformation of equation (1) is most readily evaluated by Heaviside's partial fractions expansion as shown in appendix B. The tail-load response as a function of time may be written as

$$\Delta L_t(t) = K_4 K_3 A_1 \omega_1 \left[ \frac{\sqrt{\varphi_1^2 + \varphi_2^2}}{\omega} e^{-\frac{b}{2}t} \sin(\omega t + \epsilon) + \frac{\sqrt{\varphi_3^2 + \varphi_4^2}}{\omega_1} e^{-b_1 \omega_1 t} \sin(\omega_1 t + \epsilon_1) \right] \quad (2)$$

A sample set of computations illustrating the procedure used is presented in appendix C.

## DISCUSSION

### Evaluation of the Damped Sine-Wave Elevator Motion

The assumption of a damped sine-wave elevator motion, in computing the design maneuvering horizontal tail load, is suggested for two reasons. First, the assumed motion is more representative of that applied in flight than the currently specified motion (fig. 1), because a pilot attempting to perform the specified maneuver will generally round off the corners, in effect applying a damped sine-wave control motion. (See reference 3.) Second, the use of a damped sine-wave elevator motion results in a simple and short solution using operational methods.

The damped sine-wave elevator motion used in the present report for computing the maneuvering horizontal tail load for the example airplane<sup>1</sup> described in reference 2 is shown in figure 1 where it is compared with the motion currently specified by the U.S. Air Force. The maximum up-elevator deflections were readily adjusted so that the design normal-acceleration-factor increment of 1.5 was just attained during the assumed maneuvers. The period of the damped sine-wave elevator motion was made equal to the duration of the specified motion since, as will be shown later,

---

<sup>1</sup>The pertinent basic data for the example airplane used in the computations of this report are presented in table I.

the frequency of the control motion has a very appreciable effect on the maneuvering tail load.

The tail-load variation computed by operational methods using equations (B4) and (B5) is compared in figure 2 with the variation computed by the numerical integration method described in reference 2. The agreement shown is good.

In view of the close agreement between the maneuvering tail loads computed by operational methods and those calculated by the currently specified numerical integration method, the suggested operational procedure, which provides a simple analytical expression for the tail load, merits consideration as an alternative method for establishing the design maneuvering load on the horizontal tail.

#### Effect of Control Frequency on the Tail-Load Increments

To determine the effect of control frequency on the tail-load increments for the example airplane described in table I, the normal-acceleration-factor and tail-load responses were computed for damped sine-wave elevator motions of varying frequency  $\omega_1$ . In addition to a frequency of 3.92 radians per second which corresponds to that of the motion specified in reference 2, frequencies of 2, 6, 8, and 10 radians per second were used.

Time histories of the elevator motions used are presented in figure 3(a). The corresponding acceleration-factor and tail-load responses are shown in figures 3(b) and 3(c), respectively. The maximum up-elevator deflections were again adjusted at each control frequency so that the design normal-acceleration-factor increment of 1.5 was just attained during each of the assumed maneuvers.

The effect of control frequency on the tail-load increments is clearly illustrated in figure 4 which presents the variation of the maximum positive and negative tail-load increments with control frequency. A similar effect has been computed for two other airplanes. This effect is expected and arises primarily from the greater elevator deflections required to attain the design normal acceleration factor (fig. 3(a)). It should be pointed out that, although the acceleration-factor and tail-load responses for a fixed maximum control deflection are a maximum when the control frequency  $\omega_1$  is in the neighborhood of the airplane short-period frequency  $\omega$  ( $\omega = 0.61$  in present example), the maximum tail loads for a given design normal acceleration factor were obtained at the highest control frequency investigated.



The results in figure 4 indicate that in designing the horizontal tail for maneuvering loads a very high control frequency  $\omega_1$  should be selected. However, there are two practical limitations to this procedure, namely, (1) availability of control and (2) physical or mechanical limitations of the pilot or boost system with regard to the control rate.<sup>2</sup> To elaborate upon this, figure 5, which presents the variation with control frequency of the maximum negative elevator deflection required and the maximum positive and negative control rates necessary to attain the design normal acceleration factor of 1.5 for the damped sine-wave elevator motion, was prepared. In the present example, the maximum control deflection available is not a critical limitation on the control frequency. On the other hand, the rate at which the pilot or pilot-boost-system combination is required to move or can move the control may limit the design control frequency to a low value. For airplanes in the class of the example airplane that are equipped with boost systems, a minimum control rate of 35° per second is specified by the U.S. Air Force for satisfactory handling qualities. On this basis, a minimum design control frequency of about 3.6 radians per second might be selected. (See fig. 5.) Available experimental data (reference 4) on airplanes of approximately the same size as the example airplane indicate that control rates of 70° per second can be attained. The corresponding design control frequency is about 5 radians per second. It is suggested that, unless statistical data of the type mentioned in footnote 2 indicate otherwise, the design control frequency be conservatively based on the maximum control rate attainable rather than on the minimum required rate from a handling qualities standpoint.

### CONCLUSIONS

The results of computations made to evaluate the assumption of a damped sine-wave elevator motion for computing the design maneuvering load on the horizontal tail and to determine the effect of control frequency on this load led to the following conclusions:

1. The maneuvering horizontal-tail-load variation computed using the damped sine-wave elevator motion compared closely with that computed by the currently specified numerical integration method of reference 2.

---

<sup>2</sup>Another factor not considered because of a scarcity of data is the probability that a certain maximum control rate would not be exceeded under operational or combat conditions for a given airplane design. If data were generally available, it would be desirable, for a specific design study, to base the design control rate or control frequency on a statistical analysis of measured control rates on a similar class airplane under operational or combat conditions.

---

The relatively simple analytical expression for the tail load obtained in the method using the damped sine-wave elevator motion suggests its use as an alternative method for establishing the design maneuvering load on the horizontal tail.

2. The tail-load response for a given design normal acceleration factor increased rapidly with an increase in control frequency indicating that in designing the horizontal tail for maneuvering tail loads a very high control frequency should be selected. In a practical case, the design control frequency may be limited by either availability of control or by physical or mechanical limitations of the pilot or pilot-boost-system combination with regard to control rate.

Ames Aeronautical Laboratory  
National Advisory Committee for Aeronautics  
Moffett Field, Calif., Oct. 29, 1952.

## APPENDIX A

TAIL-LOAD RESPONSE IN  $s$  PLANE

The longitudinal equations of motion for an airplane, neglecting changes in forward speed and some of the higher-order derivatives, may be written as

$$-mV\dot{\gamma} = Z_{\alpha}\Delta\alpha + Z_{\delta}\Delta\delta \quad (A1)$$

$$I_y\ddot{\theta} = M_{\alpha}\Delta\alpha + M_{\dot{\alpha}}\dot{\alpha} + M_{\dot{\theta}}\dot{\theta} + M_{\delta}\Delta\delta \quad (A2)$$

Equations (A1) and (A2) may be reduced to the equivalent second-order differential equation

$$\ddot{\alpha} + b\dot{\alpha} + k\Delta\alpha = C_0\Delta\delta + C_1\dot{\delta} \quad (A3)$$

by using the relationships (see fig. 6)

$$\theta = (\alpha_0 + \Delta\alpha) + (\gamma_0 + \Delta\gamma)$$

$$\dot{\theta} = \dot{\alpha} + \dot{\gamma}$$

$$\ddot{\theta} = \ddot{\alpha} + \ddot{\gamma}$$

In equation (A3)

$$b = \left( \frac{-Z_{\alpha}}{mV} - \frac{M_{\dot{\alpha}} + M_{\dot{\theta}}}{I_y} \right)$$

$$k = \left( \frac{-M_{\alpha}}{I_y} + \frac{Z_{\alpha}M_{\dot{\theta}}}{I_y mV} \right)$$

$$C_0 = \left( \frac{M_{\delta}}{I_y} - \frac{M_{\dot{\theta}}Z_{\delta}}{I_y mV} \right)$$

$$C_1 = \left( \frac{Z_{\delta}}{mV} \right)$$

The Laplace transformation of equation (A3), neglecting the  $\dot{\delta}$  term which is generally small and assuming initial values of  $\Delta\alpha$ ,  $\dot{\alpha}$ ,  $\ddot{\alpha}$ , and  $\Delta\delta$  are zero, may be expressed as

$$s^2\Delta\alpha(s) + bs\Delta\alpha(s) + k\Delta\alpha(s) = C_0\Delta\delta(s)$$

or

$$\Delta\alpha(s) = \frac{C_o \Delta\delta(s)}{s^2 + bs + k} \quad (A4)$$

$$\Delta A_z(s) = \frac{C_{L\alpha} q S}{W} \Delta\alpha(s) = \frac{C_{L\alpha} q C_o \Delta\delta(s)}{(W/S)(s^2 + bs + k)} \quad (A5)$$

$$\dot{\alpha}(s) = \frac{C_o s \Delta\delta(s)}{s^2 + bs + k} \quad (A6)$$

Since the maneuvering tail load may, from reference 1, be given as

$$\Delta L_t(t) = K_4 [K_1 \Delta\alpha(t) + K_2 \dot{\alpha}(t) + K_3 \Delta\delta(t)]$$

then

$$\Delta L_t(s) = K_4 [K_1 \Delta\alpha(s) + K_2 \dot{\alpha}(s) + K_3 \Delta\delta(s)] \quad (A7)$$

where

$$K_1 = \left( 1 - \frac{d\epsilon}{d\alpha} + \frac{dC_{L_t}}{d\alpha} \frac{\rho S l_t}{2m\sqrt{\eta_t}} \right)$$

$$K_2 = \left[ \frac{l_t}{V} \left( \frac{d\epsilon}{d\alpha} + \frac{1}{\sqrt{\eta_t}} \right) \right]$$

$$K_3 = \frac{d\alpha_t}{d\delta}$$

$$K_4 = \left[ \left( \frac{dC_{L_t}}{d\alpha_t} \right) \eta_t q S_t \right]$$

Substituting equations (A4) and (A6) into (A7), we have

$$\Delta L_t(s) = K_4 K_3 \left[ \frac{s^2 + \left( b + \frac{K_2 C_o}{K_3} \right) s + \left( k + \frac{K_1 C_o}{K_3} \right)}{s^2 + bs + k} \right] \Delta\delta(s) \quad (A8)$$

Equation (A8), divided through by  $\Delta\delta(s)$ , is known as the tail-load transfer function. To obtain the tail-load response in the  $s$  plane, it is simply necessary to multiply the tail-load transfer function by the Laplace transformation of  $\Delta\delta(t)$ . The damped sine-wave elevator motion is assumed to be given by the equation

$$\Delta\delta(t) = A_1 e^{-b_1 \omega_1 t} \sin \omega_1 t$$

where

$A_1$  1.39  $\Delta\delta_{\max}$

$b_1$  0.22 (damping constant required to simulate pull-up push-down design maneuver)<sup>3</sup>

$\omega_1$  control frequency

The tail-load response in the  $s$  plane may now be written as

$$\Delta L_t(s) = K_4 K_3 \left[ \frac{s^2 + \left(b + \frac{K_2 C_0}{K_3}\right)s + \left(k + \frac{K_1 C_0}{K_3}\right)}{s^2 + bs + k} \right] \left[ \frac{A_1 \omega_1}{s^2 + 2b_1 \omega_1 s + (1 + b_1^2) \omega_1^2} \right] \quad (A9)$$

Since the design tail load is generally computed for a certain design normal acceleration factor, it is also necessary to determine the acceleration-factor response which may be given in the  $s$  plane as

$$\Delta A_z(s) = \left[ \frac{C_{L_\alpha} q C_0}{(W/S)(s^2 + bs + k)} \right] \left[ \frac{A_1 \omega_1}{s^2 + 2b_1 \omega_1 s + (1 + b_1^2) \omega_1^2} \right] \quad (A10)$$

---

<sup>3</sup>In order to simulate the pull-up push-down maneuver (damping to one-half amplitude in one-half cycle) for an arbitrary control frequency, it was necessary to define the damping coefficient for the elevator motion in terms of the control frequency.

---

## APPENDIX B

## TAIL-LOAD RESPONSE IN TIME PLANE

The tail-load response as a function of time is most readily obtained by evaluating the inverse transformation of equation (A9) using Heaviside's partial fractions expansion. (See reference 5.)

By completing the square in  $s$  in the quadratic factors in the denominator, equation (A9) may be written as

$$\Delta L_t(s) = K_4 K_3 A_1 \omega_1 \left\{ \frac{s^2 + \left(b + \frac{K_2 C_0}{K_3}\right)s + \left(k + \frac{K_1 C_0}{K_3}\right)}{[(s + \frac{b}{2})^2 + \omega^2] [(s + b_1 \omega_1)^2 + \omega_1^2]} \right\} \quad (B1)$$

Equation (B1) can be written

$$\Delta L_t(s) = K_4 K_3 A_1 \omega_1 \left[ \frac{\varphi(s)}{(s + \frac{b}{2})^2 + \omega^2} \right] = K_4 K_3 A_1 \omega_1 \left[ \frac{As + b}{(s + \frac{b}{2})^2 + \omega^2} + h(s) \right] \quad (B2)$$

where  $h(s)$  represents the sum of the partial fractions corresponding to the quadratic factor  $[(s + b_1 \omega_1)^2 + \omega_1^2]$ . Multiplying through by the quadratic factor  $[(s + \frac{b}{2})^2 + \omega^2]$  and letting  $s$  approach  $-\frac{b}{2} + \omega i$

$$\varphi(-\frac{b}{2} + \omega i) = (-\frac{b}{2} + \omega i) A + B = \varphi_1 + i\varphi_2 \quad (B3)$$

where  $\varphi_1$  and  $\varphi_2$  are the real and imaginary parts of the complex quantity  $\varphi(-\frac{b}{2} + \omega i)$ .

Equating real and imaginary parts in equation (B3),

$$A = \frac{\varphi_2}{\omega}$$

$$B = \varphi_1 + \frac{Ab}{2} = \varphi_1 + \frac{\varphi_2 b}{2\omega}$$

The partial fraction corresponding to the quadratic factor is then

$$\frac{\frac{1}{\omega} [(s + \frac{b}{2}) \varphi_2 + \omega \varphi_1]}{(s + \frac{b}{2})^2 + \omega^2}$$

and the corresponding terms obtained from a table of transforms are

$$\frac{1}{\omega} e^{-\frac{b}{2}t} (\varphi_2 \cos \omega t + \varphi_1 \sin \omega t)$$

which may be written

$$\frac{1}{\omega} \sqrt{\varphi_1^2 + \varphi_2^2} e^{-\frac{b}{2}t} \sin(\omega t + \epsilon)$$

where  $\tan \epsilon = \varphi_2 / \varphi_1$ .

In a similar manner, the partial fractions expansion corresponding to the quadratic factor  $[(s+b_1\omega_1)^2 + \omega_1^2]$  may be obtained and is

$$\frac{1}{\omega_1} e^{-b_1\omega_1 t} (\varphi_4 \cos \omega_1 t + \varphi_3 \sin \omega_1 t)$$

or

$$\frac{1}{\omega_1} \sqrt{\varphi_3^2 + \varphi_4^2} e^{-b_1\omega_1 t} \sin(\omega_1 t + \epsilon_1)$$

where  $\tan \epsilon_1 = \varphi_4 / \varphi_3$ .

The complete expansion is the sum of the two expansions and may be written as

$$\Delta L_t(t) = K_4 K_3 A_1 \omega_1 \left[ \frac{e^{-\frac{b}{2}t}}{\omega} (\varphi_2 \cos \omega t + \varphi_1 \sin \omega t) + \frac{e^{-b_1\omega_1 t}}{\omega_1} (\varphi_4 \cos \omega_1 t + \varphi_3 \sin \omega_1 t) \right]$$

or

$$\Delta L_t(t) = K_4 K_3 A_1 \omega_1 \left[ \frac{\sqrt{\varphi_1^2 + \varphi_2^2}}{\omega} e^{-\frac{b}{2}t} \sin(\omega t + \epsilon) + \frac{\sqrt{\varphi_3^2 + \varphi_4^2}}{\omega_1} e^{-b_1\omega_1 t} \sin(\omega_1 t + \epsilon_1) \right] \quad (B4)$$

In a similar manner, the normal-acceleration-factor response in the time plane may be determined to be

$$\Delta A_Z(t) = \frac{C_{L\alpha} q C_O A_1 \omega_1}{W/S} \left[ \frac{\sqrt{\varphi_5^2 + \varphi_6^2}}{\omega} e^{-\frac{b}{2}t} \sin(\omega t + \epsilon_2) + \frac{\sqrt{\varphi_7^2 + \varphi_8^2}}{\omega_1} e^{-b_1 \omega_1 t} \sin(\omega_1 t + \epsilon_3) \right] \quad (B5)$$

where  $\tan \epsilon_2 = \varphi_6 / \varphi_5$  and  $\tan \epsilon_3 = \varphi_8 / \varphi_7$ . The main problem in evaluating the expansions (B4) and (B5) resolves itself into determining the values of  $\varphi$ . For convenience, the relationships (which are perfectly general if a damped sine-wave elevator motion is assumed) of  $\varphi_1 \dots \varphi_8$  in terms of known constants are provided below:

$$\varphi_1 = \frac{FR + GS}{R^2 + S^2}; \quad \varphi_2 = \frac{GR - FS}{R^2 + S^2}$$

where

$$F = \frac{K_1 C_O}{K_3} - \frac{b K_2 C_O}{2 K_3}$$

$$G = \frac{\omega K_2 C_O}{K_3}$$

$$R = \frac{b^2}{4} - \omega^2 - b_1 \omega_1 b + (1 + b_1^2) \omega_1^2$$

$$S = 2b_1 \omega_1 \omega - b\omega$$

$$\varphi_3 = \frac{F_1 R_1 + G_1 S_1}{R_1^2 + S_1^2}; \quad \varphi_4 = \frac{G_1 R_1 - F_1 S_1}{R_1^2 + S_1^2}$$

where

$$F_1 = b_1^2 \omega_1^2 - \omega_1^2 - b b_1 \omega_1 - \frac{b_1 \omega_1 K_2 C_O}{K_3} + \frac{K_1 C_O}{K_3} + k$$

$$G_1 = b \omega_1 + \frac{K_2 C_O \omega_1}{K_3} - 2b_1 \omega_1^2$$

$$R_1 = b_1^2 \omega_1^2 - \omega_1^2 - b b_1 \omega_1 + k$$

$$S_1 = b \omega_1 - 2b_1 \omega_1^2$$



$$\varphi_5 = \frac{R}{R^2+S^2}; \quad \varphi_6 = \frac{-S}{R^2+S^2}$$

and

$$\varphi_7 = \frac{R_1}{R_1^2+S_1^2}; \quad \varphi_8 = \frac{-S_1}{R_1^2+S_1^2}$$

## APPENDIX C

## EXAMPLE COMPUTATIONS

To illustrate the method described in appendixes A and B, the tail-load and acceleration-factor responses to a damped sine-wave elevator motion using the example airplane described in reference 2 will be computed. The geometric and aerodynamic characteristics of the airplane are given in table I.

The pertinent aerodynamic derivatives and airplane constants are determined as follows:

$$Z_{\alpha} = -C_{L_{\alpha}} q S = -(5.14)(131)(1457) = -980,000$$

$$Z_{\delta} = -C_{L_{\delta}} q S = -(0.437)(131)(1457) = -83,500$$

$$M_{\alpha} = C_{m_{\alpha}} q S \bar{c} = -(0.3131)(131)(1457)(13.64) = -815,000$$

$$M_{q_t} = \eta_t C_{L_{t\alpha_t}} \frac{\rho V S_t l_t^2}{2} = - \frac{(0.834)(4.10)(0.0015)(325)(48.682)^2}{2} = -823,000$$

$$M_q = K M_{q_t} = (1.25)(-823,000) = -1,030,000$$

$$M_{\alpha}^* = M_{q_t} \frac{d\epsilon}{d\alpha} = -(823,000)(0.40) = -329,000$$

$$M_{\delta} = C_{m_{\delta}} q S \bar{c} = -(1.56)(131)(1457)(13.64) = -4,060,000$$

$$b = \frac{-Z_{\alpha}}{mV} - \frac{M_q}{I_y} - \frac{M_{\alpha}^*}{I_y}$$

$$b = \frac{980,000}{(1925)(417)} + \frac{1,030,000}{560,730} + \frac{329,000}{560,730} = 3.64$$

$$k = - \frac{M_{\alpha}}{I_y} + \frac{Z_{\alpha} M_q}{I_y mV}$$

$$k = \frac{815,000}{560,730} + \frac{(980,000)(1,030,000)}{(560,730)(1925)(417)} = 3.68$$

$$c_o = \frac{M_{\delta}}{I_y} - \frac{M_q Z_{\delta}}{I_y mV}$$

$$C_0 = \frac{-4,060,000}{560,730} - \frac{(-1,030,000)(-83,500)}{(560,730)(1925)(417)} = -7.43$$

$$C_1 = \frac{Z_0}{mV} = \frac{-83,500}{(1925)(417)} = -0.104$$

For simplicity,  $C_1$  is omitted from subsequent analysis because it is relatively small compared to other coefficients.

$$K_1 = 1 - \frac{d\epsilon}{d\alpha} + C_{L\alpha} \frac{\rho S l_t}{2m\sqrt{\eta_t}}$$

$$K_1 = 1 - 0.40 + (5.14) \frac{(0.0015)(1457)(48.682)}{2(1925)(0.913)} = 0.756$$

$$K_2 = \frac{l_t}{V} \left( \frac{d\epsilon}{d\alpha} + \frac{1}{\sqrt{\eta_t}} \right)$$

$$K_2 = \frac{48.682}{417} \left( 0.40 + \frac{1}{0.913} \right) = 0.1744$$

$$K_3 = \frac{d\alpha_t}{d\delta} = 0.478$$

$$K_4 = C_{L_t \alpha_t} \eta_t q S_t$$

$$K_4 = (4.10)(0.834)(131)(325) = 145,700$$

A damped sine-wave control motion given by the equation

$$\Delta\delta = -1.39e^{-(0.22)(3.92)t} \sin 3.92t$$

was assumed where the values of the damping coefficient  $b_1$  and the control frequency  $\omega_1$  were adjusted to simulate the specified motion described in reference 2. The values of  $\phi$  may be obtained from the relationships provided in appendix B as follows:

$$\phi_1 = \frac{FR+GS}{R^2+S^2} = \frac{(-6.82)(15.91) + (-1.65)(-1.167)}{(15.91)^2 + (-1.167)^2} = -0.419$$

$$\phi_2 = \frac{GR-FS}{R^2+S^2} = \frac{(-1.65)(15.91)-(-6.82)(-1.167)}{(15.91)^2 + (-1.167)^2} = -0.135$$

$$\phi_3 = \frac{F_1R_1+G_1S_1}{R_1^2+S_1^2} = \frac{(-23.495)(-14.115)+(-3.12)(7.50)}{(-14.115)^2 + (7.50)^2} = 1.207$$

$$\phi_4 = \frac{G_1R_1-F_1S_1}{R_1^2+S_1^2} = \frac{(-3.12)(-14.115)-(-23.495)(7.50)}{(-14.115)^2 + (7.50)^2} = 0.862$$

$$\phi_5 = \frac{R}{R^2+S^2} = \frac{15.91}{(15.91)^2 + (-1.167)^2} = 0.0623$$

$$\phi_6 = \frac{-S}{R^2+S^2} = \frac{-(-1.167)}{(15.91)^2 + (-1.167)^2} = 0.00457$$

$$\phi_7 = \frac{R_1}{R_1^2+S_1^2} = \frac{-14.115}{(-14.115)^2 + (7.50)^2} = -0.0551$$

$$\phi_8 = \frac{-S_1}{R_1^2+S_1^2} = \frac{-7.50}{(-14.115)^2 + (7.50)^2} = -0.0294$$

Referring to equations (B4) and (B5), the tail-load and acceleration-factor responses in the time plane may be written, respectively, as

$$\Delta L_t(t) = -380,000 \left[ 0.721e^{-1.82t} \sin(0.61t + 3.453) + 0.379e^{-0.882t} \sin(3.92t + 0.62) \right] \quad (C1)$$

$$\Delta A_Z(t) = 640 \left[ 0.1025e^{-1.82t} \sin(0.61t + 0.0734) + 0.016e^{-0.882t} \sin(3.92t + 3.632) \right] \quad (C2)$$

For convenience, equations (C1) and (C2) are given for a peak control deflection  $\Delta\delta_{\max}$  of -1.0 radian. After one set of computations the tail loads and the control deflections may be scaled down so that the design normal acceleration factor is just attained in the maneuver. The computational procedure for obtaining the normal acceleration factor and the maneuvering tail-load increments is presented in tables II and III, respectively. The results scaled down to the design normal-acceleration-factor increment of 1.5 are included in figure 3 for a control frequency  $\omega_1$  of 3.92 radians per second.

## REFERENCES

1. Pearson, Henry A.: Derivation of Charts for Determining the Horizontal Tail Load Variation with Any Elevator Motion. NACA Rep. 759, 1943.
2. Kelley, Joseph, Jr., and Missall, John W.: Maneuvering Horizontal Tail Loads. Army Air Forces, Air Tech. Service Command Wright Field, Tech. Rep. 5185, 1945.
3. Sadoff, Melvin, and Clousing, Lawrence A.: Measurements of the Pressure Distribution on the Horizontal-Tail Surface of a Typical Propeller-Driven Pursuit Airplane in Flight. III - Tail Loads in Abrupt Pull-Up Push-Down Maneuvers. NACA TN 1539, 1948.
4. Matheny, Cloyce E.: Maximum Pitching Angular Accelerations of Airplanes Measured in Flight. NACA TN 2103, 1950.
5. Churchill, Ruel V.: Modern Operational Mathematics in Engineering. McGraw-Hill, N.Y., 1944, pp. 41-51.

TABLE I.- PERTINENT BASIC DATA FOR EXAMPLE AIRPLANE USED IN THE COMPUTATIONS

Airplane weight, $W$ , pounds. . . . .	62,000
Airplane mass ( $W/g$ ), slugs . . . . .	1,925
Airplane pitching moment of inertia, $I_y$ , slug-feet squared. . . . .	560,730
Wing area, $S$ , square feet. . . . .	1,457
Horizontal-tail area, $S_t$ , square feet. . . . .	324.88
Wing mean aerodynamic chord, $\bar{c}$ , feet . . . . .	13.64
Horizontal-tail length, $l_t$ , feet . . . . .	48.682
Airplane lift-curve slope, $Cl_\alpha$ , per radian. . . . .	5.14
Horizontal-tail lift-curve slope, $(Cl_\alpha)_t$ , per radian. . . . .	4.10
Airplane stability parameter, $C_{m_\alpha}$ , per radian. . . . .	-0.3131
Elevator moment effectiveness, $C_{m_\delta}$ , per radian . . . . .	-1.56
Relative elevator-stabilizer effectiveness ( $d\alpha_t/d\delta$ ) . . . . .	0.478
Downwash factor ( $d\epsilon/d\alpha$ ). . . . .	0.400
Ratio of horizontal tail to wing dynamic pressure ( $q_t/q$ ). . . . .	0.834
Pressure altitude, $h_p$ , feet . . . . .	15,000
Mass density of air, $\rho$ , slugs per cubic foot. . . . .	0.0015
Airplane velocity, $V$ , feet per second. . . . .	417
Design normal-acceleration-factor increment ( $AZ_{max}-1$ ). . . . .	1.5
Center-of-gravity location, percent $\bar{c}$ . . . . .	38

TABLE II.- NORMAL ACCELERATION FACTOR CALCULATIONS

1	2	3	4	5	6	7	8	9	10	11	12	13	14	15	16	17
Row	t	$-\frac{b}{2} \textcircled{2}$	$e \textcircled{3}$	$\omega \textcircled{2}$	$e \textcircled{3} + \omega \textcircled{2}$	$\sin \textcircled{6}$	$0.1025 \times \textcircled{4} \times \textcircled{7}$	$-b_1 \omega_1 \textcircled{2}$	$e \textcircled{3}$	$\omega_1 \textcircled{2}$	$\omega_1 \textcircled{2} + e \textcircled{3}$	$\sin \textcircled{12}$	$0.016 \times \textcircled{10} \times \textcircled{13}$	$e \textcircled{3} + \textcircled{14}$	$640 \textcircled{15}$	$^1 \Delta A_z$
1	0	0	1.00	0	0.0734	0.0734	0.00732	0	1.00	0	3.632	-0.469	-0.00752	0	0	0
2	.1	-.182	.834	.061	.1344	.134	.01147	-.0863	.916	.392	4.024	-.772	-.0113	.00017	.109	.01
3	.2	-.364	.693	.122	.1954	.194	.0138	-.1727	.840	.784	4.416	-.960	-.0129	.0009	.576	.08
4	.3	-.546	.578	.183	.2564	.254	.01507	-.259	.772	1.177	4.809	-.995	-.0123	.00277	1.773	.24
5	.4	-.728	.482	.244	.3174	.312	.01543	-.3455	.707	1.569	5.201	-.88	-.00995	.00548	3.507	.47
6	.5	-.910	.401	.305	.3784	.370	.01522	-.4315	.648	1.962	5.594	-.636	-.00659	.00863	5.523	.74
7	.6	-1.092	.335	.366	.4394	.425	.01460	-.518	.595	2.355	5.987	-.292	-.00278	.01182	7.565	1.02
8	.7	-1.273	.280	.427	.5004	.481	.01380	-.604	.547	2.744	6.376	.0977	.000855	.014655	9.379	1.26
9	.8	-1.456	.233	.488	.5614	.532	.01272	-.691	.501	3.136	6.768	.469	.00377	.01649	10.554	1.42
10	.9	-1.638	.194	.549	.6224	.582	.01160	-.777	.459	3.53	7.162	.778	.00572	.01732	11.085	1.50
11	1.0	-1.82	.162	.610	.6834	.631	.01050	-.863	.422	3.92	7.552	.957	.00646	.01696	10.854	1.46
12	1.1	-2.00	.135	.671	.7444	.677	.00935	-.949	.387	4.32	7.952	.995	.00617	.01552	9.933	1.34
13	1.2	-2.185	.112	.732	.8054	.721	.00827	-1.037	.355	4.71	8.342	.883	.00502	.01329	8.506	1.14
14	1.3	-2.365	.094	.793	.8664	.762	.00735	-1.122	.325	5.09	8.722	.643	.00334	.01069	6.842	.92
15	1.4	-2.55	.078	.854	.9274	.800	.00640	-1.210	.298	5.49	9.122	.292	.00139	.00779	4.986	.67
16	1.5	-2.73	.065	.915	.9884	.835	.00557	-1.296	.274	5.88	9.512	-.0872	-.000382	.005188	3.320	.45
17	1.6	-2.915	.054	.976	1.0494	.866	.00479	-1.382	.251	6.27	9.902	-.469	-.00189	.00290	1.856	.25

Note:  $b/2 = 1.82$   
 $\omega = 0.61$

$e_2 = 0.0734$   
 $e_3 = 3.632$

$b_1 = 0.22$   
 $\omega_1 = 3.92$

$$\frac{\sqrt{e_2^2 + e_3^2}}{\omega} = 0.1025$$

$$\frac{\sqrt{e_7^2 + e_8^2}}{\omega_1} = 0.016$$

<sup>1</sup>Values in column 17 obtained by multiplying column 16 by ratio  $\frac{1.5}{11.085}$

TABLE III.- MANEUVERING TAIL-LOAD CALCULATIONS

1	2	3	4	5	6	7	8	9	10	11	12	13	14	15	16	17
Row	t	$-\frac{b}{2} \textcircled{2}$	$e \textcircled{3}$	$w \textcircled{2}$	$\textcircled{5} + e$	$\sin \textcircled{6}$	$0.721 \times \textcircled{4} \times \textcircled{7}$	$-b_1 w_1 \textcircled{2}$	$e \textcircled{8}$	$w_1 \textcircled{2}$	$\textcircled{11} + e_1$	$\sin \textcircled{12}$	$0.379 \times \textcircled{10} \times \textcircled{13}$	$\textcircled{8} + \textcircled{14}$	$-380,000 \times \textcircled{15}$	$^1 \Delta L_t$
1	0	0	1.00	0	3.453	-0.306	-0.220	0	1.00	0	0.620	0.581	0.220	0	0	0
2	.1	-.182	.834	.061	3.514	-.364	-.219	-.0863	.916	.392	1.012	.848	.294	.075	-28,550	-3,860
3	.2	-.364	.693	.122	3.575	-.420	-.210	-.1727	.840	.784	1.404	.986	.313	.103	-39,200	-5,310
4	.3	-.546	.578	.183	3.636	-.475	-.198	-.259	.772	1.177	1.797	.974	.284	.086	-32,700	-4,430
5	.4	-.728	.482	.244	3.697	-.527	-.183	-.3455	.707	1.569	2.189	.815	.218	.035	-13,300	-1,800
6	.5	-.910	.401	.305	3.758	-.578	-.167	-.4315	.648	1.962	2.582	.531	.130	-.037	14,100	1,910
7	.6	-1.092	.335	.366	3.819	-.627	-.152	-.518	.595	2.355	2.975	.166	.037	-.115	43,700	5,920
8	.7	-1.273	.280	.427	3.880	-.673	-.136	-.604	.547	2.744	3.364	-.221	-.046	-.182	69,200	9,370
9	.8	-1.456	.233	.488	3.941	-.717	-.120	-.691	.501	3.136	3.756	-.576	-.109	-.229	87,200	11,800
10	.9	-1.638	.194	.549	4.002	-.758	-.106	-.777	.459	3.53	4.150	-.846	-.147	-.253	96,200	13,000
11	1.0	-1.82	.162	.610	4.063	-.796	-.093	-.863	.422	3.92	4.540	-.985	-.157	-.250	95,100	12,880
12	1.1	-2.00	.135	.671	4.124	-.832	-.081	-.949	.387	4.32	4.940	-.974	-.143	-.224	85,200	11,530
13	1.2	-2.185	.112	.732	4.185	-.864	-.070	-1.037	.355	4.71	5.330	-.815	-.110	-.180	68,500	9,270
14	1.3	-2.365	.094	.793	4.246	-.893	-.060	-1.122	.325	5.09	5.710	-.542	-.067	-.127	48,300	6,540
15	1.4	-2.55	.078	.854	4.307	-.919	-.052	-1.210	.298	5.49	6.110	-.172	-.019	-.071	27,000	3,660
16	1.5	-2.73	.065	.915	4.368	-.941	-.044	-1.296	.274	5.88	6.500	.215	.022	-.022	8,360	1,130
17	1.6	-2.915	.054	.976	4.429	-.960	-.037	-1.382	.251	6.27	6.890	.570	.054	.017	-6,460	-875

Note:  $b/2 = 1.82$   
 $w = 0.61$

$e = 3.453$   
 $e_1 = 0.62$

$b_1 = 0.22$   
 $w_1 = 3.92$

$$\frac{\sqrt{\phi_1^2 + \phi_2^2}}{w} = 0.721$$

$$\frac{\sqrt{\phi_8^2 + \phi_4^2}}{w_1} = 0.379$$



<sup>1</sup>Values in column 17 obtained by multiplying values in column 16 by ratio 1.5/11.085 (See table II.)





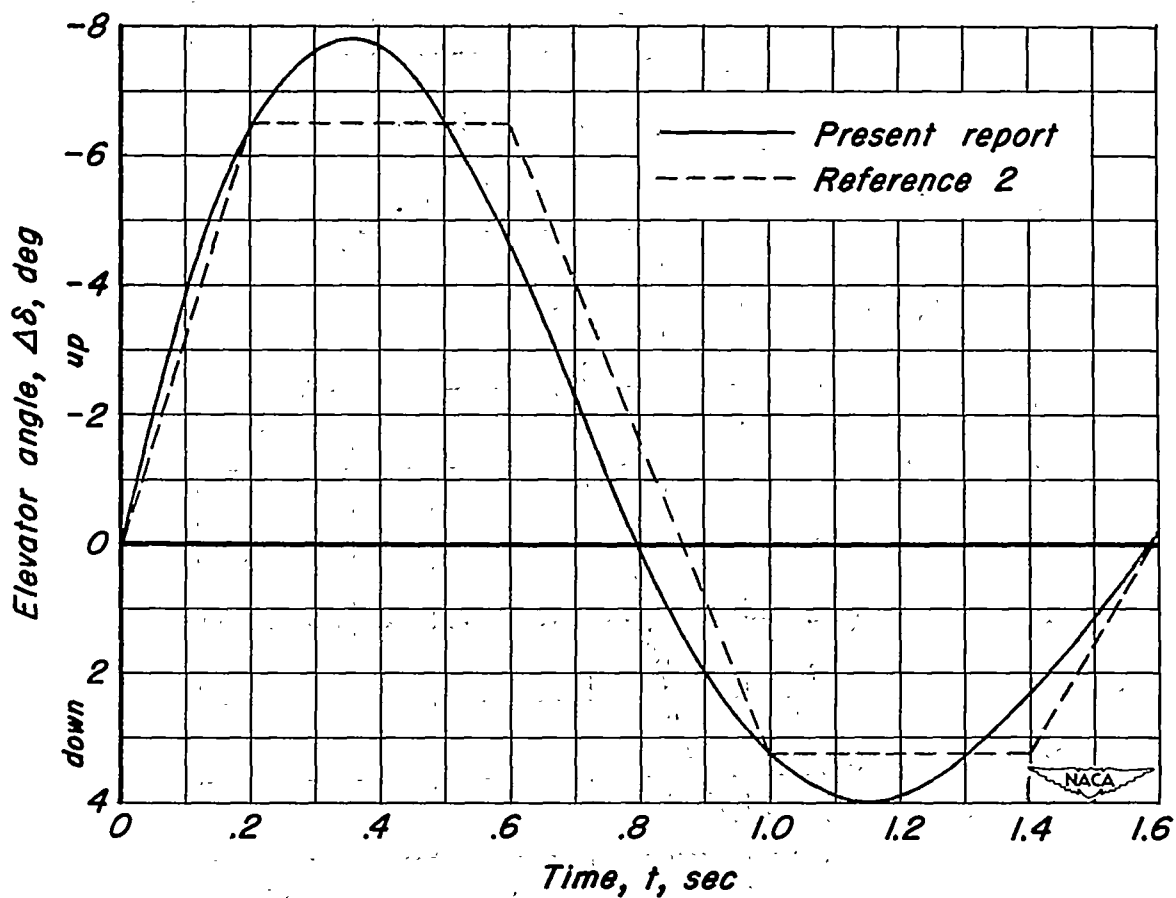


Figure 1.— Comparison of the damped sine-wave elevator motion with the motion used in the method of reference 2.

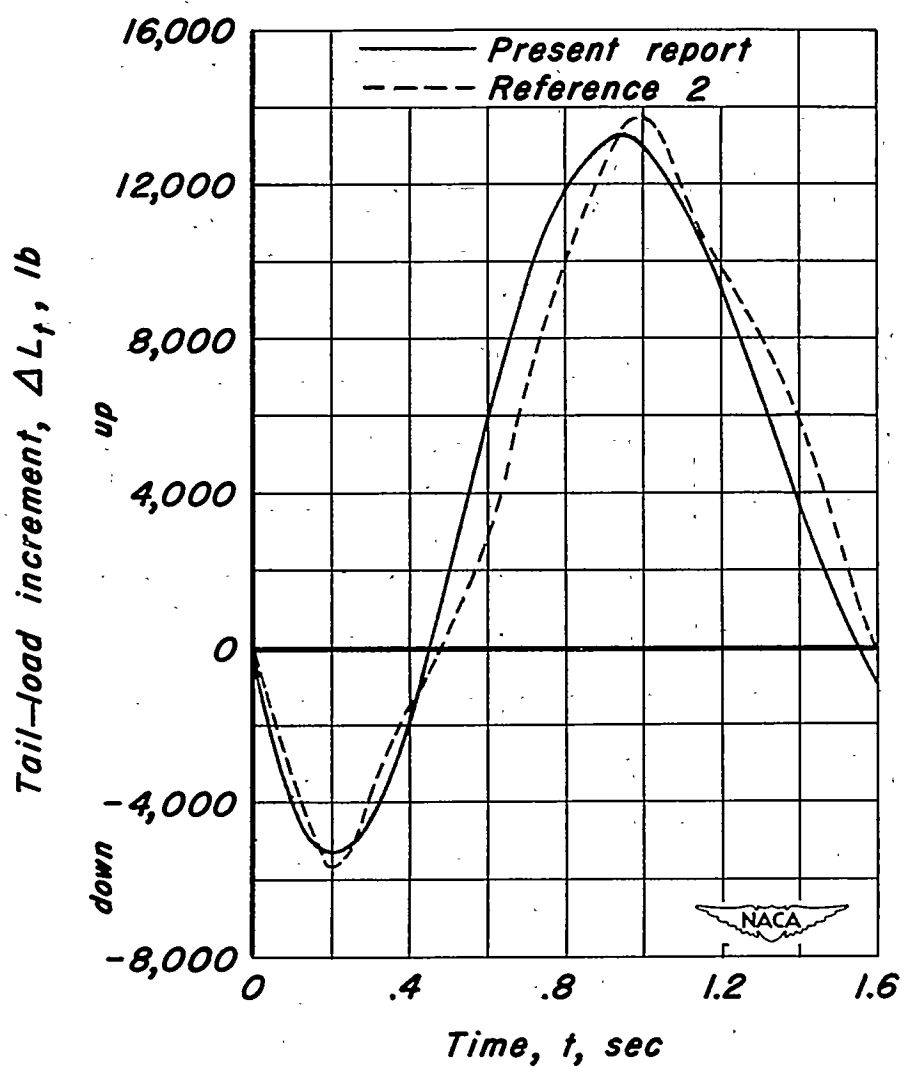
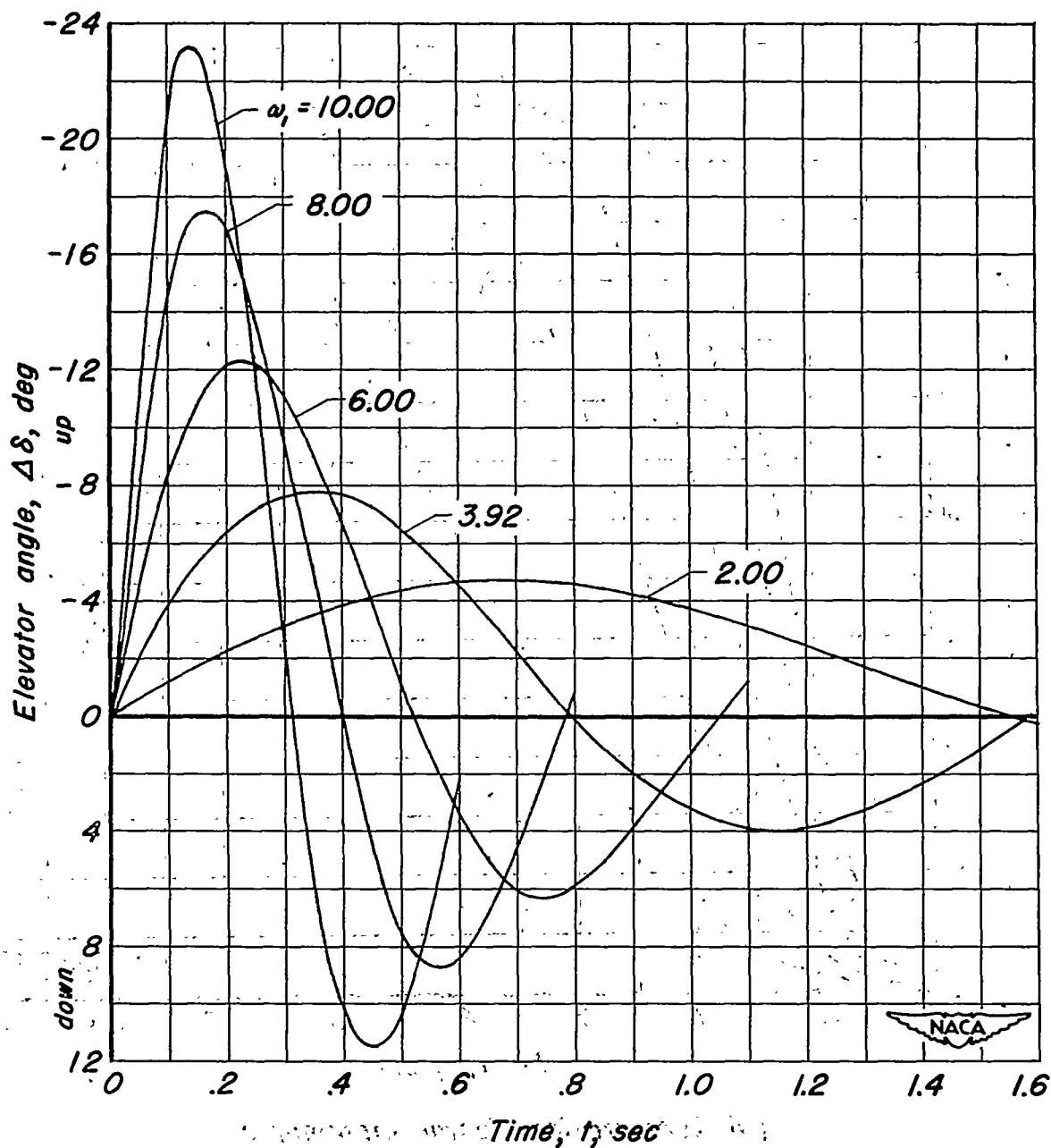
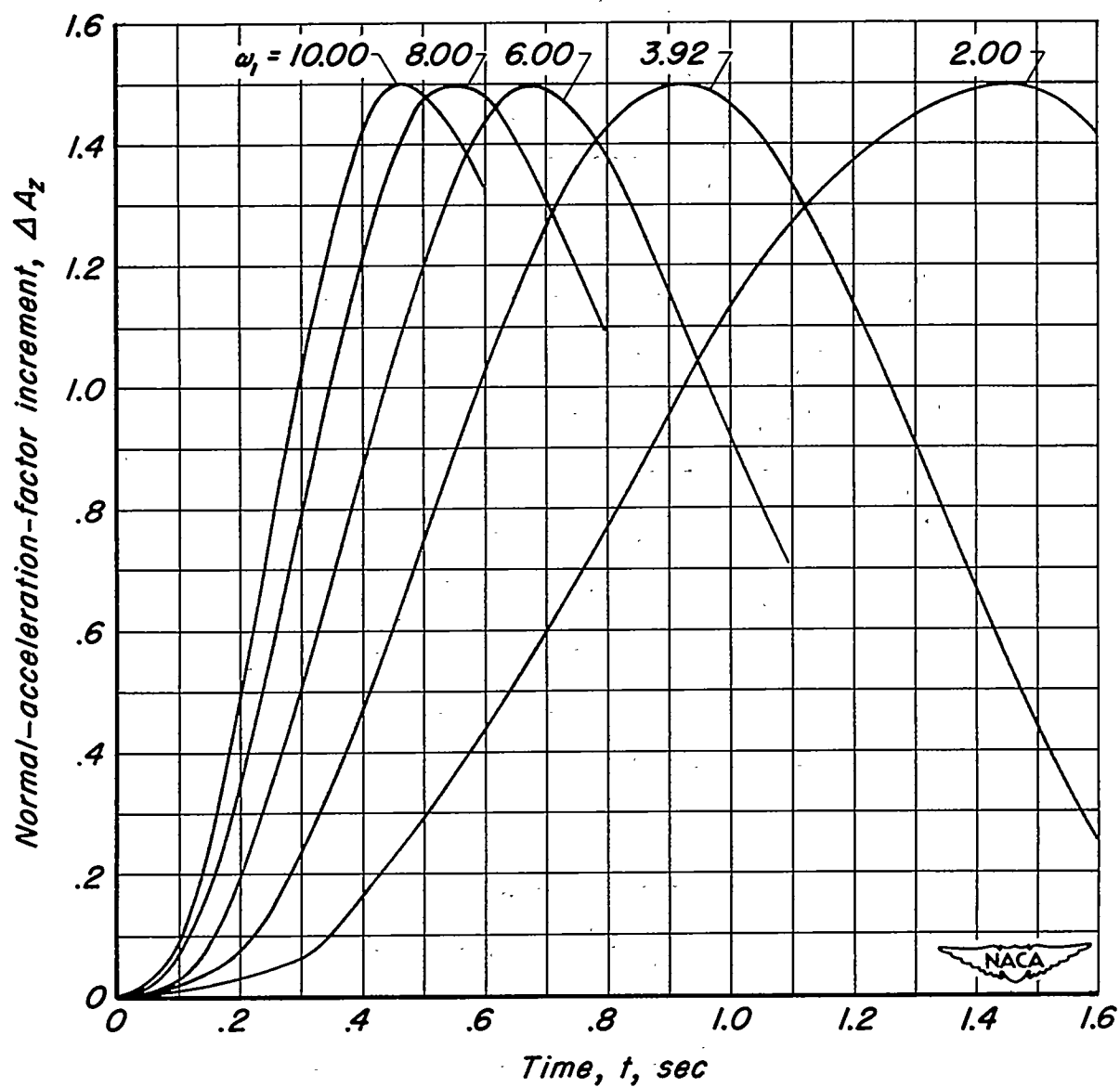


Figure 2.— Comparison of the tail-load variation computed by the methods of the present report with that computed by the method of reference 2.



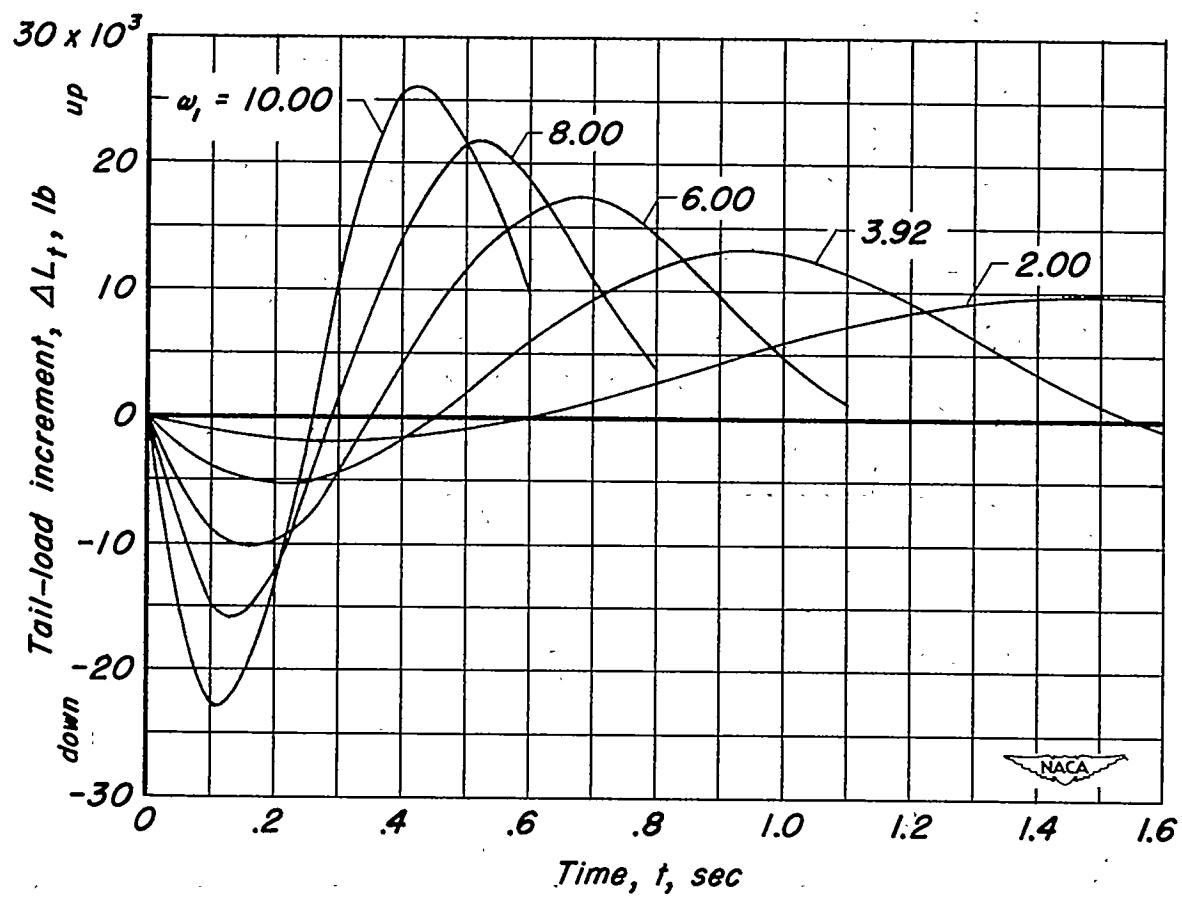
(a) Elevator-deflection increments.

Figure 3.- Computed time histories of elevator deflection, normal-acceleration-factor and tail-load increments for several values of control frequency  $\omega_1$ .



(b) Acceleration-factor increments.

Figure 3.- Continued.



(c) Tail-load increments.

Figure 3.—Concluded.

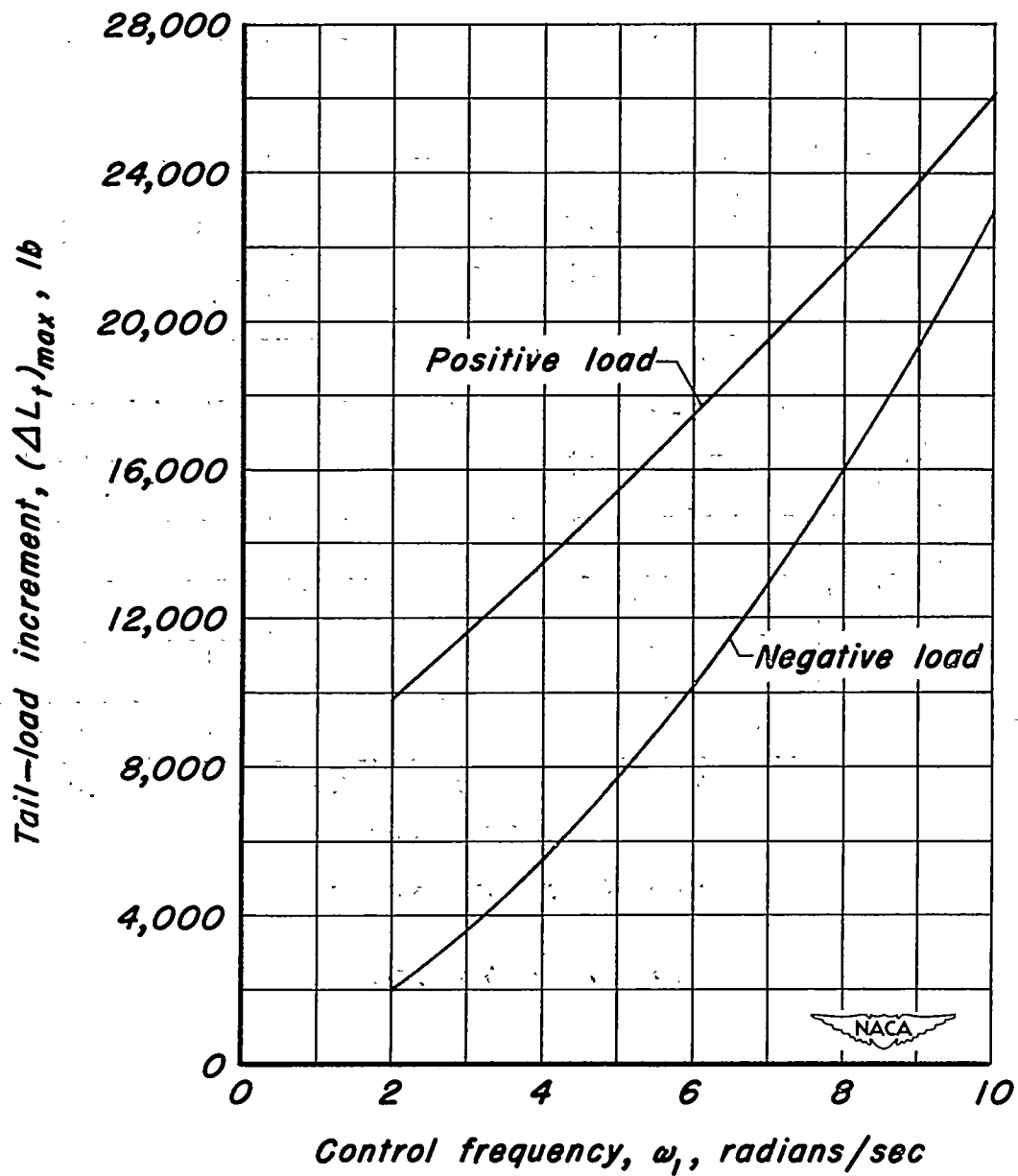


Figure 4.—Variation with control frequency  $\omega_1$  of the maximum positive and negative tail-load increments for a maximum acceleration-factor increment of 1.5.

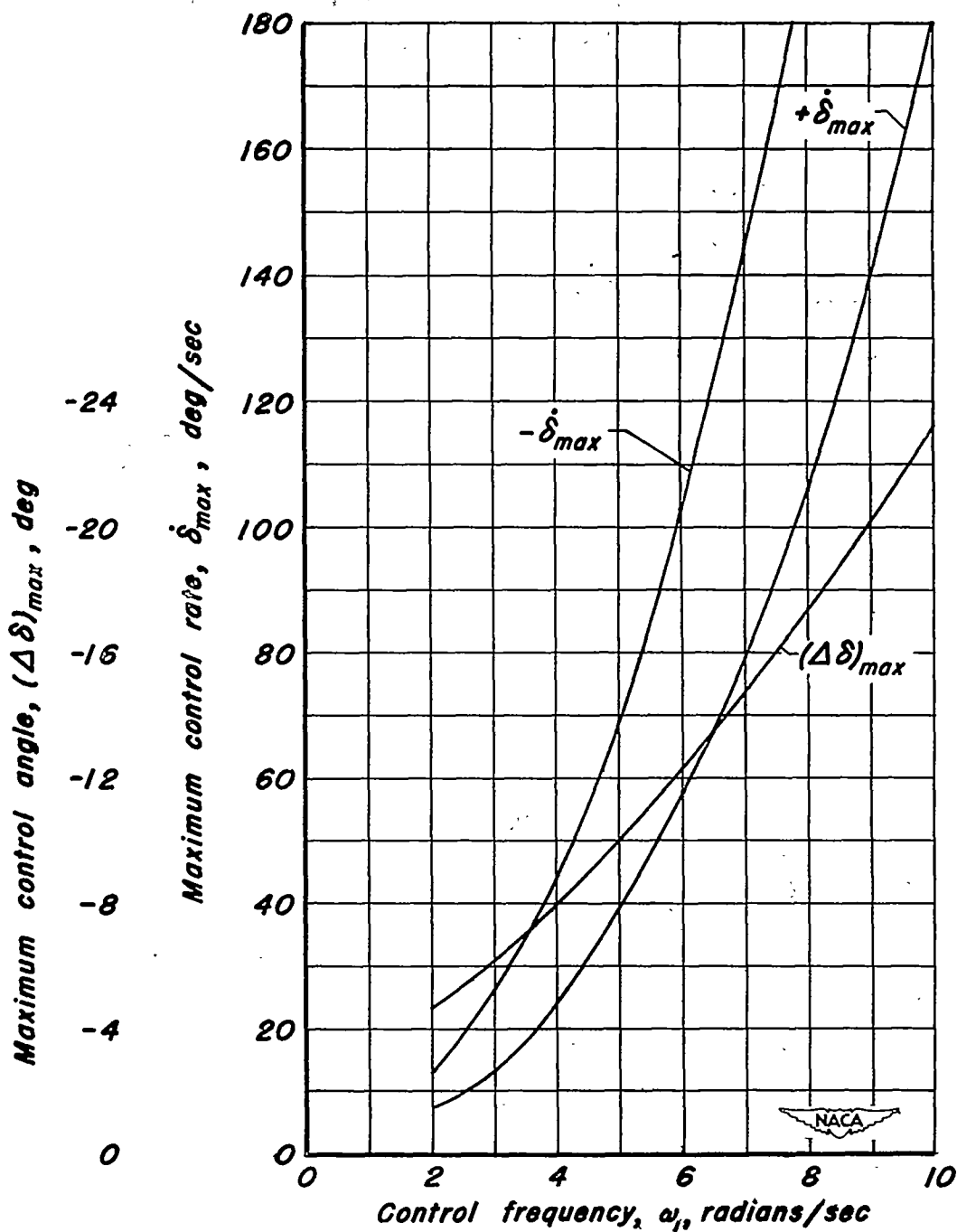
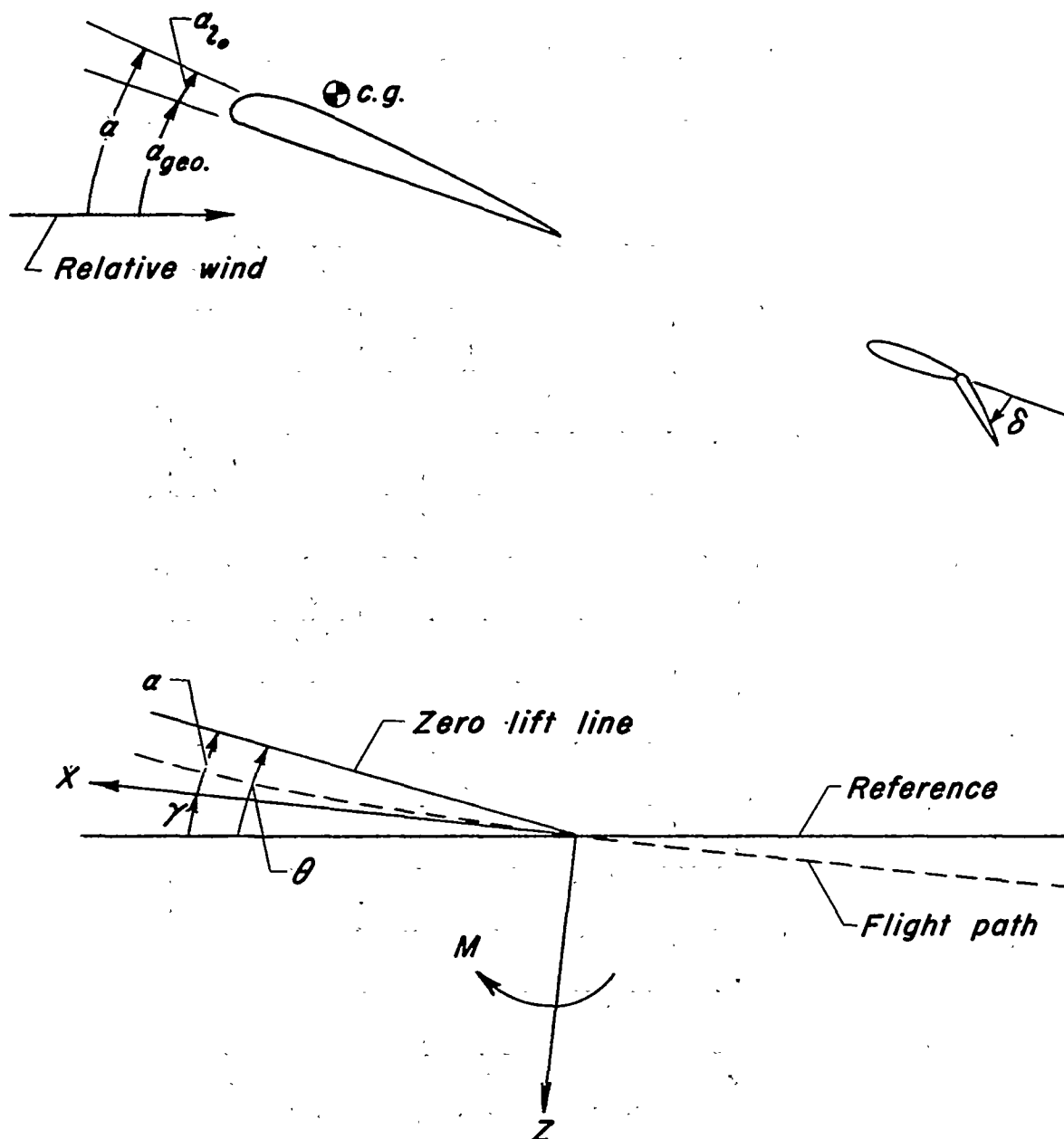


Figure 5.— Effect of control frequency,  $\omega$ , on the maximum control deflection and on the maximum positive and negative control rates required for a maximum positive acceleration factor increment of 1.5.



**Note: Positive directions and angles shown.  
X axis tangent to flight path.**



**Figure 6.— Sign conventions and pertinent geometric relationships.**

